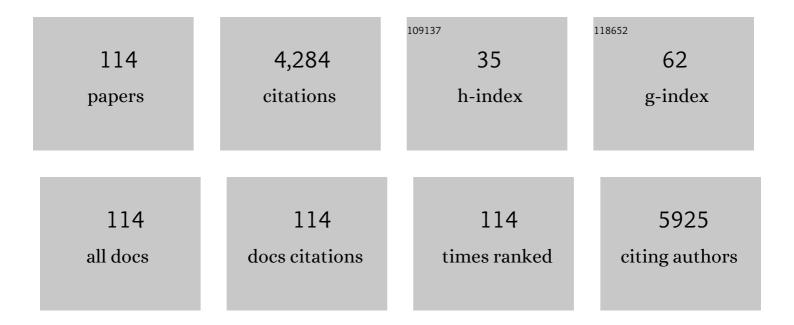
List of Publications by Year in descending order

Source: https://exaly.com/author-pdf/6978968/publications.pdf Version: 2024-02-01



FUNC YEOD KIM

#	Article	IF	CITATIONS
1	kâ€ŧ FOCUSS: A general compressed sensing framework for high resolution dynamic MRI. Magnetic Resonance in Medicine, 2009, 61, 103-116.	1.9	536
2	Self-Confirming "AND―Logic Nanoparticles for Fault-Free MRI. Journal of the American Chemical Society, 2010, 132, 11015-11017.	6.6	270
3	Improvedk–tBLAST andk–tSENSE using FOCUSS. Physics in Medicine and Biology, 2007, 52, 3201-3226.	1.6	235
4	MR Imaging of Metronidazole-Induced Encephalopathy: Lesion Distribution and Diffusion-Weighted Imaging Findings. American Journal of Neuroradiology, 2007, 28, 1652-1658.	1.2	234
5	Morphological alterations in the congenital blind based on the analysis of cortical thickness and surface area. NeuroImage, 2009, 47, 98-106.	2.1	201
6	Mitochondrial respiratory chain defects: Underlying etiology in various epileptic conditions. Epilepsia, 2008, 49, 685-690.	2.6	129
7	Quantitative susceptibility mapping using deep neural network: QSMnet. NeuroImage, 2018, 179, 199-206.	2.1	115
8	Motor pathway injury in patients with periventricular leucomalacia and spastic diplegia. Brain, 2011, 134, 1199-1210.	3.7	113
9	Acute Diverticulitis of the Cecum and Ascending Colon. American Journal of Roentgenology, 2000, 174, 1397-1402.	1.0	96
10	Acceleration of MR parameter mapping using annihilating filterâ€based low rank hankel matrix (ALOHA). Magnetic Resonance in Medicine, 2016, 76, 1848-1864.	1.9	83
11	Dysplastic Nodules in Liver Cirrhosis: Evaluation of Hemodynamics with CT during Arterial Portography and CT Hepatic Arteriography. Radiology, 2000, 214, 869-874.	3.6	82
12	Nigrosome 1 Detection at 3T MRI for the Diagnosis of Early-Stage Idiopathic Parkinson Disease: Assessment of Diagnostic Accuracy and Agreement on Imaging Asymmetry and Clinical Laterality. American Journal of Neuroradiology, 2015, 36, 2010-2016.	1.2	81
13	Detection of Thrombus in Acute Ischemic Stroke. Stroke, 2005, 36, 2745-2747.	1.0	75
14	CT Sign of Brain Swelling without Concomitant Parenchymal Hypoattenuation: Comparison with Diffusion- and Perfusion-weighted MR Imaging. Radiology, 2005, 235, 992-998.	3.6	74
15	Time-Dependent Thrombus Resolution After Tissue-Type Plasminogen Activator in Patients With Stroke and Mice. Stroke, 2015, 46, 1877-1882.	1.0	71
16	Nonspecific interstitial pneumonia with fibrosis: serial high-resolution CT findings with functional correlation American Journal of Roentgenology, 1999, 173, 949-953.	1.0	70
17	Prediction of hemorrhagic transformation in acute ischemic stroke: role of diffusion-weighted imaging and early parenchymal enhancement. American Journal of Neuroradiology, 2005, 26, 1050-5.	1.2	69
18	Regenerative Nodules in Liver Cirrhosis: Findings at CT during Arterial Portography and CT Hepatic Arteriography with Histopathologic Correlation. Radiology, 1999, 210, 451-458.	3.6	63

#	Article	IF	CITATIONS
19	Prediction of thrombolytic efficacy in acute ischemic stroke using thin-section noncontrast CT. Neurology, 2006, 67, 1846-1848.	1.5	63
20	lmaging of nigrosome 1 in substantia nigra at 3T using multiecho susceptibility mapâ€weighted imaging (SMWI). Journal of Magnetic Resonance Imaging, 2017, 46, 528-536.	1.9	60
21	Drug-induced Parkinsonism versus Idiopathic Parkinson Disease: Utility of Nigrosome 1 with 3-T Imaging. Radiology, 2016, 279, 849-858.	3.6	54
22	Contrast-enhanced, three-dimensional, whole-brain, black-blood imaging: Application to small brain metastases. Magnetic Resonance in Medicine, 2010, 63, 553-561.	1.9	51
23	Exploring linearity of deep neural network trained QSM: QSMnet+. NeuroImage, 2020, 211, 116619.	2.1	49
24	Interstitial Pneumonia in Progressive Systemic Sclerosis: Serial High-Resolution CT Findings with Functional Correlation. Journal of Computer Assisted Tomography, 2001, 25, 757-763.	0.5	47
25	Dysfunctional modulation of emotional interference in the medial prefrontal cortex in patients with schizophrenia. Neuroscience Letters, 2008, 440, 119-124.	1.0	47
26	ldiopathic Synovial Osteochondromatosis of the Hip: Radiographic and MR Appearances in 15 Patients. Korean Journal of Radiology, 2002, 3, 254.	1.5	45
27	Intramuscular vascular malformations of an extremity: findings on MR imaging and pathologic correlation. Skeletal Radiology, 1999, 28, 515-521.	1.2	43
28	Computer-Aided Detection of Metastatic Brain Tumors Using Magnetic Resonance Black-Blood Imaging. Investigative Radiology, 2013, 48, 113-119.	3.5	43
29	Magnetic resonance findings of primary central nervous system tâ€cell lymphoma in immunocompetent patients. Acta Radiologica, 2005, 46, 187-192.	0.5	42
30	Detection of Small Metastatic Brain Tumors. Investigative Radiology, 2012, 47, 136-141.	3.5	41
31	An Investigation of Lateral Geniculate Nucleus Volume in Patients With Primary Open-Angle Glaucoma Using 7 Tesla Magnetic Resonance Imaging. , 2014, 55, 3468.		41
32	Reorganization of neural circuits in the blind on diffusion direction analysis. NeuroReport, 2007, 18, 1757-1760.	0.6	40
33	Mechanisms of <i>T</i> <sub>2</sub> * anisotropy and gradient echo myelin water imaging. NMR in Biomedicine, 2017, 30, e3513.	1.6	40
34	Diagnosis of Early-Stage Idiopathic Parkinson's Disease Using High-Resolution Quantitative Susceptibility Mapping Combined with Histogram Analysis in the Substantia Nigra at 3 T. Journal of		

#	Article	IF	CITATIONS
37	Computed Tomography-Based Thrombus Imaging for the Prediction of Recanalization after Reperfusion Therapy in Stroke. Journal of Stroke, 2017, 19, 40-49.	1.4	36
38	Infantile Fibromatosis in Childhood: Findings on MR Imaging and Pathologic Correlation. Clinical Radiology, 2000, 55, 19-24.	0.5	35
39	Ultrasonographic evaluation of focal hepatic lesions: comparison of pulse inversion harmonic, tissue harmonic, and conventional imaging techniques Journal of Ultrasound in Medicine, 2000, 19, 293-299.	0.8	32
40	Nigrosome 1 imaging: technical considerations and clinical applications. British Journal of Radiology, 2019, 92, 20180842.	1.0	29
41	Multiphasic Perfusion Computed Tomography in Hyperacute Ischemic Stroke: Comparison with Diffusion and Perfusion Magnetic Resonance Imaging. Journal of Computer Assisted Tomography, 2003, 27, 194-206.	0.5	28
42	Thrombus Volume Comparison between Patients with and without Hyperattenuated Artery Sign on CT. American Journal of Neuroradiology, 2008, 29, 359-362.	1.2	28
43	Three dimension double inversion recovery gray matter imaging using compressed sensing. Magnetic Resonance Imaging, 2010, 28, 1395-1402.	1.0	28
44	Differential involvement of nigral subregions in idiopathic parkinson's disease. Human Brain Mapping, 2018, 39, 542-553.	1.9	28
45	Intra-Arterial Thrombolytic Therapy for Hyperacute Ischemic Stroke Caused by Tandem Occlusion. Cerebrovascular Diseases, 2008, 26, 184-189.	0.8	27
46	Acute occlusion of the middle cerebral artery: early evaluation with triphasic helical CTpreliminary results Radiology, 1998, 207, 113-122.	3.6	26
47	Sulcal Hyperintensity on Fluid-Attenuated Inversion Recovery Imaging in Acute Ischemic Stroke Patients Treated With Intra-Arterial Thrombolysis. Journal of Computer Assisted Tomography, 2005, 29, 264-269.	0.5	25
48	Assessment of regional GABAA receptor binding using 18F-fluoroflumazenil positron emission tomography in spastic type cerebral palsy. NeuroImage, 2007, 34, 19-25.	2.1	25
49	Extranodal nasal-type NK/T-cell lymphoma: Computed tomography findings of head and neck involvement. Acta Radiologica, 2010, 51, 164-169.	0.5	25
50	Ischemic Stroke: Measurement of Intracranial Artery Calcifications Can Improve Prediction of Asymptomatic Coronary Artery Disease. Radiology, 2013, 268, 842-849.	3.6	24
51	Prediction of thrombus resolution after intravenous thrombolysis assessed by CT-based thrombus imaging. Thrombosis and Haemostasis, 2012, 107, 786-794.	1.8	21
52	Triple-Layer Appearance of Brodmann Area 4 at Thin-Section Double Inversion-Recovery MR Imaging. Radiology, 2009, 250, 515-522.	3.6	20
53	Neuroradiologic findings in children with mitochondrial disorder: correlation with mitochondrial respiratory chain defects. European Radiology, 2008, 18, 1741-1748.	2.3	19
54	Multiphase MR Angiography Collateral Map: Functional Outcome after Acute Anterior Circulation Ischemic Stroke. Radiology, 2020, 295, 192-201.	3.6	17

#	Article	IF	CITATIONS
55	Overlapping Ablation Using a Coaxial Radiofrequency Electrode and Multiple Cannulae System: Experimental Study in ex-Vivo Bovine Liver. Korean Journal of Radiology, 2003, 4, 117.	1.5	16
56	Visualization of maturation of the corpus callosum during childhood and adolescence using T2 relaxometry. International Journal of Developmental Neuroscience, 2007, 25, 409-414.	0.7	16
57	Temporal Bone CT Findings in Cornelia de Lange Syndrome. American Journal of Neuroradiology, 2008, 29, 569-573.	1.2	16
58	Measuring Fractional Anisotropy of the Corpus Callosum Using Diffusion Tensor Imaging: Mid-Sagittal versus Axial Imaging Planes. Korean Journal of Radiology, 2008, 9, 391.	1.5	16
59	A Novel Collateral Imaging Method Derived from Time-Resolved Dynamic Contrast-Enhanced MR Angiography in Acute Ischemic Stroke: A Pilot Study. American Journal of Neuroradiology, 2019, 40, 946-953.	1.2	16
60	Continuous Conversion of CT Kernel Using Switchable CycleGAN With AdaIN. IEEE Transactions on Medical Imaging, 2021, 40, 3015-3029.	5.4	16
61	Automated assessment of the substantia nigra on susceptibility map-weighted imaging using deep convolutional neural networks for diagnosis of Idiopathic Parkinson's disease. Parkinsonism and Related Disorders, 2021, 85, 84-90.	1.1	15
62	Simple microwire and microcatheter mechanical thrombolysis with adjuvant intraarterial urokinase for treatment of hyperacute ischemic stroke patients. Acta Radiologica, 2008, 49, 351-357.	0.5	14
63	Intracranial Dural Metastasis of Ewing's Sarcoma: a Case Report. Korean Journal of Radiology, 2008, 9, 76.	1.5	14
64	Quantification of intracranial internal carotid artery calcification on brain unenhanced CT: evaluation of its feasibility and assessment of the reliability of visual grading scales. European Radiology, 2013, 23, 20-27.	2.3	14
65	Wholeâ€brain perfusion imaging with balanced steadyâ€state free precession arterial spin labeling. NMR in Biomedicine, 2016, 29, 264-274.	1.6	14
66	Pseudoaneurysm of the Inferior Thyroid Artery Presenting as a Thyroid Nodule. Thyroid, 2009, 19, 69-71.	2.4	13
67	Tuberculous Encephalopathy without Meningitis: Pathology and Brain MRI Findings. European Neurology, 2011, 65, 156-159.	0.6	13
68	SENSE factors for reliable cortical thickness measurement. NeuroImage, 2008, 40, 187-196.	2.1	12
69	A Mobile Tele-Radiology Imaging System with JPEG2000 for an Emergency Care. Journal of Digital Imaging, 2011, 24, 709-718.	1.6	12
70	Comparison of Imaging Selection Criteria for Intra-Arterial Thrombectomy in Acute Ischemic Stroke with Advanced CT. European Radiology, 2016, 26, 2974-2981.	2.3	12
71	Initial diagnostic workup of parkinsonism: Dopamine transporter positron emission tomography versus susceptibility map-weighted imaging at 3T. Parkinsonism and Related Disorders, 2019, 62, 171-178.	1.1	12
72	Primary Peripheral T-Cell Lymphoma of the Face Other Than Mycosis Fungoides. Journal of Computer Assisted Tomography, 2004, 28, 670-675.	0.5	11

#	Article	IF	CITATIONS
73	Early Recurring Hepatocellular Carcinoma after Partial Hepatic Resection: Preoperative CT Findings. Korean Journal of Radiology, 2000, 1, 38.	1.5	10
74	Unpaired Training of Deep Learning tMRA for Flexible Spatio-Temporal Resolution. IEEE Transactions on Medical Imaging, 2021, 40, 166-179.	5.4	10
75	Earlyâ€stage Parkinson's disease: Abnormal nigrosome 1 and 2 revealed by a voxelwise analysis of neuromelaninâ€sensitive <scp>MRI</scp> . Human Brain Mapping, 2021, 42, 2823-2832.	1.9	10
76	Imaging-Based Management of Acute Ischemic Stroke Patients: Current Neuroradiological Perspectives. Korean Journal of Radiology, 2015, 16, 372.	1.5	9
77	Thrombus imaging in acute ischaemic stroke using thin-slice unenhanced CT: comparison of conventional sequential CT and helical CT. European Radiology, 2012, 22, 2392-2396.	2.3	8
78	Susceptibility-resistant variable-flip-angle turbo spin echo imaging for reliable estimation of cortical thickness: A feasibility study. NeuroImage, 2012, 59, 377-388.	2.1	8
79	Phaseâ€sensitive, dualâ€acquisition, singleâ€slab, 3D, turboâ€spinâ€echo pulse sequence for simultaneous <i>T</i> <sub>2</sub> â€weighted and fluidâ€attenuated wholeâ€brain imaging. Magnetic Resonance in Medicine, 2010, 63, 1422-1430.	1.9	7
80	Intraoperative Frozen Cytology of Central Nervous System Neoplasms: An Ancillary Tool for Frozen Diagnosis. Journal of Pathology and Translational Medicine, 2019, 53, 104-111.	0.4	7
81	A prospective multi-centre study of susceptibility map-weighted MRI for the diagnosis of neurodegenerative parkinsonism. European Radiology, 2022, 32, 3597-3608.	2.3	7
82	Hippocampal sclerosis and encephalomalacia as prognostic factors of tuberculous meningitis-related and herpes simplex encephalitis-related epilepsy. Seizure: the Journal of the British Epilepsy Association, 2011, 20, 570-574.	0.9	6
83	Pediatric intracerebral histiocytic sarcoma with rhabdoid features: Case report and literature review. Neuropathology, 2017, 37, 560-568.	0.7	6
84	Crush Cytology of Microcystic Meningioma with Extensive Sclerosis. Korean Journal of Pathology, 2014, 48, 77.	1.2	6
85	Review of the Current Status of Intra-Arterial Thrombolysis for Treating Acute Cerebral Infarction: a Retrospective Analysis of the Data from Multiple Centers in Korea. Korean Journal of Radiology, 2007, 8, 87.	1.5	5
86	Dynamic Contrast-Enhanced MR Angiography Exploiting Subspace Projection for Robust Angiogram Separation. IEEE Transactions on Medical Imaging, 2017, 36, 584-595.	5.4	5
87	Mapping cerebral perfusion from time-resolved contrast-enhanced MR angiographic data. Magnetic Resonance Imaging, 2019, 61, 143-148.	1.0	5
88	Prefrontal functional dissociation in the semantic network of patients with schizophrenia. NeuroReport, 2008, 19, 1391-1395.	0.6	4
89	Cinical Application of Iopamidol (Pamiray® 300) for Cerebral Angiography. Journal of the Korean Radiological Society, 2007, 57, 121.	0.0	4
90	Rapid wholeâ€brain gray matter imaging using singleâ€slab threeâ€dimensional dualâ€echo fast spin echo: A feasibility study. Magnetic Resonance in Medicine, 2017, 78, 1691-1699.	1.9	3

#	Article	IF	CITATIONS
91	Signal Alteration in the Optic Nerve Head on 3D T2-weighted MRI: a Potential Neuroimaging Sign of Glaucomatous Optic Neuropathy. Current Eye Research, 2018, 43, 397-405.	0.7	3
92	3D Multi-Scale Residual Network Toward Lacunar Infarcts Identification From MR Images With Minimal User Intervention. IEEE Access, 2021, 9, 11787-11797.	2.6	3
93	A Deep Learning-Based Automatic Collateral Assessment in Patients with Acute Ischemic Stroke. Translational Stroke Research, 2023, 14, 66-72.	2.3	3
94	On the use of a spinâ€echo based double inversion recovery acquisition for the measurement of cortical brain thickness. Journal of Magnetic Resonance Imaging, 2011, 33, 1218-1223.	1.9	2
95	Retrospective multiâ€phase nonâ€contrastâ€enhanced magnetic resonance angiography (ROMANCE MRA) for robust angiogram separation in the presence of cardiac arrhythmia. Magnetic Resonance in Medicine, 2018, 80, 976-989.	1.9	2
96	Cortical thinning pattern according to differential nigrosome involvement in patients with Parkinson's disease. NeuroImage: Clinical, 2020, 28, 102382.	1.4	2
97	Granulomatous angiopanniculitis of the breast: mammographic and sonographic findings Journal of Ultrasound in Medicine, 1999, 18, 519-521.	0.8	1
98	T2 prime mapping from highly undersampled data using compressed sensing with patch based low rank penalty. , 2014, , .		1
99	Improved temporal resolution of twist imaging using annihilating filter-based low rank Hankel matrix approach. , 2016, , .		1
100	The Impact of Discrepancy between Measured versus Stated Weight on Hemorrhagic Transformation and Clinical Outcomes after Intravenous Alteplase Thrombolysis. Cerebrovascular Diseases, 2017, 44, 241-247.	0.8	1
101	Perfusion Maps Acquired From Dynamic Angiography <scp>MRI</scp> Using Deep Learning Approaches. Journal of Magnetic Resonance Imaging, 0, , .	1.9	1
102	On the use of a spin-echo based double inversion recovery acquisition for the measurement of cortical brain thickness. Journal of Magnetic Resonance Imaging, 2011, 33, spcone-spcone.	1.9	0
103	T2 Relaxation Times of the Cingulate Cortex, Amygdaloid Body, Hippocampal Body, and Insular Cortex: Comparison of 1.5 T and 3.0 T. Journal of the Korean Society of Magnetic Resonance in Medicine, 2011, 15, 67.	0.1	0
104	Single Subcortical Infarct: Pathomechanism Assessed by Thin-Section Computed Tomography Perfusion. Journal of Stroke and Cerebrovascular Diseases, 2017, 26, 1440-1448.	0.7	0
105	Regarding "Perfusion MR Imaging Using a 3D Pulsed Continuous Arterial Spin-Labeling Method for Acute Cerebral Infarction Classified as Branch Atheromatous Disease Involving the Lenticulostriate Artery Territory― American Journal of Neuroradiology, 2017, 38, E103-E103.	1.2	0
106	Improved Time-Resolved MRA Using k-Space Deep Learning. Lecture Notes in Computer Science, 2018, , 47-54.	1.0	0
107	Is High-Spatial-Resolution Diffusion MRI Applicable for the Diagnosis of Parkinson Disease?. Radiology, 2019, 292, 267-268.	3.6	0
108	Interlinking brain mapping and Parkinson's disease: MRI analysis, nigrosome 1 and nigrosome 4. , 2020, , 267-281.		0

267-281.

#	Article	IF	CITATIONS
109	Do the Magic Angle Effects or Susceptibility Effects Affect the Visualization of Nigrosome 1?. American Journal of Neuroradiology, 2020, 41, E20-E20.	1.2	0
110	A Case of Supratentorial Intra-axial Ependymoma Showing Exophytic Growth. Journal of the Korean Radiological Society, 2007, 57, 419.	0.0	0
111	High Resolution Time Resolved Contrast Enhanced MR Angiography Using k-t FOCUSS. Journal of the Korean Society of Magnetic Resonance in Medicine, 2010, 14, 10.	0.1	0
112	Phalangeal and Metacarpal Metastases from Clear Cell Sarcoma of the Kidney: A Case Report. Journal of the Korean Radiological Society, 1998, 39, 1233.	0.0	0
113	Pulmonary Hemosiderosis Due to Mitral Valvular Heart Disease. Journal of the Korean Radiological Society, 1999, 40, 73.	0.0	0
114	Bronchiectasis: Diagnostic Accuracy of Chest Computed Radiography. Journal of the Korean Radiological Society, 1999, 40, 871.	0.0	0